Effect of Li- and Ta-doping on the ferroelectric properties of $Na_{0.5}K_{0.5}NbO_3$ thin films prepared by a chelate route

A. Fernández Solarte, N. Pellegri, O. de Sanctis & M. G. Stachiotti

Journal of Sol-Gel Science and Technology

ISSN 0928-0707
Volume 66
Number 3

J Sol-Gel Sci Technol (2013) 66:488-496
DOI 10.1007/s10971-013-3036-3

Springer

J Sol-Gel Sci Technol (2013) 66:488–496
DOI 10.1007/s10971-013-3036-3

ORIGINAL PAPER

Effect of Li- and Ta-doping on the ferroelectric properties of $Na_{0.5}K_{0.5}NbO_3$ thin films prepared by a chelate route

A. Fernández Solarte · N. Pellegri · O. de Sanctis · M. G. Stachiotti

Received: 12 January 2013 / Accepted: 9 April 2013 / Published online: 19 April 2013

Abstract The effects of lithium and tantalum doping on the properties of $Na_{0.5}K_{0.5}NbO_3$ (NKN) thin films were investigated. The films were fabricated by an optimized chelate route which offers the advantage of a simple and rapid solution synthesis. The optimization was achieved by investigating the effects of alkaline volatilization loss on film properties. In this way, undoped NKN thin films fabricated by this conventional method exhibited good ferroelectric properties ($P_r \sim 8$ μC/cm^2, and $E_c \sim 55$ kV/cm for films annealed at 650 °C). The developed chelate route was then used to grow Li (5 %) and Ta (10 %) substituted thin films. Such structures allowed us to compare the effect of these dopant cations on phase formation, microstructure and ferroelectric properties. We show that both modifications produced a remarkable improvement on the ferroelectricity of the films. While the undoped material exhibited large leakage components in films annealed at 600 °C, films modified with Li or Ta presented well saturated ferroelectric hysteresis loops, indicating that those ions have a significant influence on the conducting process. The remnant polarizations of the Ta-doped films are greater than those of the Li-doped samples. This feature is however reversed for films annealed at low temperature (600 °C) due to the presence of a non-ferroelectric secondary phase in the Ta-doped composition.

A. F. Solarte · N. Pellegri · O. de Sanctis
Laboratorio de Materiales Cerámicos, Universidad Nacional de Rosario, IFIR, CONICET, Av. Pellegrini 250, S2000BTP Rosario, Argentina

M. G. Stachiotti (✉)
Instituto de Física Rosario, Universidad Nacional de Rosario, 27 de Febrero 210 Bis (2000), Rosario, Argentina
e-mail: stachiotti@ifir-conicet.gov.ar

Keywords Ferroelectric thin films · Lead-free piezoelectrics · Sol–Gel

1 Introduction

Lead-based ferroelectric materials such as $Pb(Zr_xTi_{1-x})O_3$ are extensively used due to their excellent dielectric, ferroelectric and piezoelectric properties. However, the high concentration of Pb in this compound has drawbacks from environmental concerns, leading to increasing attention on lead-free candidates [1–6]. Between them, $Na_{0.5}K_{0.5}NbO_3$ (NKN) based ceramics are one of the most promising, due to their relatively good piezoelectric properties and high Curie temperature. However, the processing of NKN ceramics is problematic owing to the high volatility of alkali species at high temperatures. Reasonable piezoelectric properties have been achieved by doping. Systems modified by $LiTaO_3$ and $LiSbO_3$ have been the most intensively studied. NKN in combination with tetragonal $LiTaO_3$ exhibits a morphotropic phase boundary between orthorhombic and tetragonal phases at $\sim$5 mol% of $LiTaO_3$ accompanied by enhancement of piezoelectric properties [7–11]. The addition of $LiSbO_3$ to pure NKN shifts the orthorhombic to tetragonal phase transition temperature down to room temperature and increases the piezoelectric d_{33} coefficient [12–14]. In the pioneering work of Saito et al. [15], for instance, optimization of the NKN by separate lithium, tantalum and antimony additions yielded a d_{33} coefficient of $\sim$300 pC/N.

NKN based materials are also interesting candidates for high performance lead-free piezoelectric thin films owing to its biocompatible nature [16]. The fabrication of NKN thin films has been reported previously by various techniques [17–21]. Films produced by chemical solution

deposition methods typically have large leakage currents and it is always difficult to obtain well-saturated polarization hysteresis loops [22]. This drawback comes out from the loss of stoichiometry because Na and K are easy to volatilize during the thermal treatment of the films. On the other hand, compositional engineering in NKN thin films are rarer than in bulk ceramics. Recently, Wang et al. [23] demonstrated that Mn-doped NKN films exhibited a low leakage current density and a well-saturated P-E hysteresis loop. Abazari et al. [24] demonstrated that Mn-doped (K, Na, Li) (Nb, Ta, Sb)O_3 thin film exhibited an effective piezoelectric coefficient d_{33} of $\sim$53 pC/N. Also, (K, Na, Li) (Nb, Ta)O_3 thin film without sintering aids were reported with improved piezoelectric properties [25–27].

In this work, Li- and Ta-substituted $Na_{0.5}K_{0.5}NbO_3$ thin films were deposited onto Pt/TiO_2/SiO_2/Si substrates by an optimized chemical solution deposition route. Such structures allowed us to compare the effect of the two dopant cations on the microstructure and ferroelectric properties of the films. For this, we first developed a chelate route for the synthesis of undoped NKN thin films which offers the advantage of simple and rapid solution synthesis; in comparison with the 2-methoxyethanol process, distillation and refluxing strategies are not required. This chelate route was optimized by investigating the effects of alkaline volatilization loss on film properties. We show that undoped NKN thin films annealed at 650 °C display a well crystallized perovskite structure with good ferroelectric properties. Then, the optimized route is used to grow Li- and Ta-substituted thin films. Phase formation, microstructure and ferroelectric properties are compared. We show that both modifications produce a remarkable improvement of the ferroelectric properties, even for films annealed at low temperature (600 °C), indicating that Li and Ta additions have a significant influence on the conducting process.

2 Experimental procedure

The choice of precursors, solvents and chelating agents is very important for producing high-quality thin films using chemical solution deposition processing based on a chelate route. Regarding the chelating agent, acetic acid, acetylacetone, or amine compounds are the most commonly use. We have shown, however, that the use of alkanolamines as chelating agent produces the segregation of metallic bismuth in as-prepared $SrBi_2Ta_2O_9$ powders [28]. The amine group is a powerful Lewis base which reduces cations during the evaporation of solvent and formation of the gel powder. α-Hydroxyketones, on the other hand, have emerged as good chelating agents due to their stabilization effects on metal alkoxides solutions. In particular, it was found that acetoin (3-Hydroxy 2-butanone) has the highest stabilization effect on Ti, Zr, Ta and Nb metal alkoxides. The utilization of acetoin in the preparation of ferroelectric thin films produces the elimination of residual organic compounds at a lower temperature and an earlier onset of crystallization [29, 30]. For that reason, the present route is based on the utilization of acetoin as chelating agent.

NKN solutions were prepared starting from sodium ethoxide, potassium ethoxide, niobium ethoxide as metal precursors; acetoin and ethanol were used as chelating agent and solvent, respectively. Firstly, Niobium pentaethoxide (Nb $(OCH_2CH_3)_5$, 99.95 % Aldrich) was dissolved in a solution of acetoin (3-hydroxy-2-butanone, Aldrich) and ethanol with a ratio [Nb (OCH_2CH_3) 5]/[acetoin] = 1/4. Afterwards, one solution of potassium ethoxide ($KOCH_2CH_3$, 24 wt% solution in ethanol, Aldrich) and subsequently another one of sodium ethoxide ($NaOCH_2CH_3$, 21 wt% solution in ethanol, Aldrich) were added to the Niobium precusor solution. Each step of the procedure was performed under a nitrogen atmosphere and a continuous stirring. Finally, water (dissolved in ethanol) was added up to reach a molar ratio $[H_2O]/[NKN] = 2$. The NKN molar concentration of the solution was equal to 0.125. Precursor solutions for the fabrication of Ta- and Li-modified thin films were prepared following the procedure described above, with the incorporation of the corresponding amounts of tantalum pentaethoxide (Ta $(OCH_2CH_3)_5$, 99.95 % Aldrich) and lithium ethoxide ($LiOCH_2CH_3$, 21 wt% solution in ethanol, Aldrich). To investigate the effects of Na and K volatilization loss on film properties, different excess amount of alkaline chemicals was added to the precursor solutions, which were prepared with a 0 mol% alkaline excess, a 10 and 20 mol% excess amount of sodium ethoxide and a 15 mol% amount of potassium ethoxide that correspond to the compositions (labeled as): $Na_{0.5}K_{0.5}NbO_3$ (NK00), $Na_{0.55}K_{0.5}NbO_3$ (N10), $Na_{0.6}K_{0.5}NbO_3$ (N20) and $Na_{0.5}K_{0.575}NbO_3$ (K15), respectively.

To grow the films, the precursor solutions were spin-coated on Pt/TiO_2/SiO_2/Si substrates at 3,000 rpm for 30 s in a clean bench. The wet films were dried at 200 °C for 7 min. Subsequently, the burning of residual groups in the films was performed at 400 °C for 10 min in air. Finally, various lots of specimens were annealed in air at temperatures between 600 and 750 °C for 5 min. For thicker films, a multilayer process was used, repeating the coating/heat-treatment cycle three times. The thickness of each sample was determined by ellipsometry using a Rudolph Ellipsometer with a wavelength of 634 nm. For instance, the thickness of a 0 mol% excess NKN three-layer film annealed at 600 °C was 235 ± 3 nm, and its refractive index was 2.074 ± 0.008. As all films were grown in similar conditions, their thicknesses are similar to the above value.

Gel powders were obtained from the precursor solution by solvent evaporation under a pressure of 40 torrs; then the obtained gels were dried at 200 °C for 24 h. Thermal analyses (DTA-TG) of the gel powders were performed using a Shimatzu DTG 60H equipment with a heating rate of 10 °C/min from room temperature to 600 °C in normal atmosphere. Crystal structures of thin films and ceramic powders were analyzed at room temperature using a Philips X'Pert Pro X-ray diffractometer with Cu K_α radiation of wavelength 1.5406 Å, at a scan rate of 0.02 °/s. For thin films, the measurements were made with grazing incident X-ray diffraction (GIXRD), using a Sollar slit to get parallel beam for diffraction. Surface morphology was observed by scanning electron microscopy using a FEI Quanta 200 FESEM Environmental, and atomic force microscopy (AFM NanoTec ELECTRONICA). To measure the electrical properties of the films, 0.3-mm-diameter Pt top electrodes were deposited by DC sputtering on the films and then annealed at 400 °C for 60 min. The Pt layer of the substrates was used as bottom electrodes. Ferroelectric properties were evaluated using a ferroelectric test system (a conventional Sawyer-Tower circuit) applying AC signals at 50 Hz at room temperature.

3 Results and discussions

3.1 Undoped $Na_{0.5}K_{0.5}NbO_3$ thin films

In this section we highlight the more relevant results obtained from a systematic investigation of the effects produced by alkaline volatilization loss on the properties of undoped NKN films. To this end, solutions with different excess amount of alkaline chemicals were prepared. Figure 1 shows the XRD patterns of thin films annealed at 600 °C (Fig. 1a) and 700 °C (Fig. 1b) fabricated from precursor solutions with 0 mol% (NK00) alkaline excess, 10 mol% (N10) and 20 mol% (N20) excess amount of sodium ethoxide, and a 15 mol% (K15) amount of potassium ethoxide. All the films exhibit diffraction peaks corresponding to the NKN perovskite phase. However, only the films derived from the 20 mol% Na excess precursor solution (N20) exhibited a spectrum free of spurious phases, with a well crystallized perovskite structure. NK00 thin films annealed at 600 °C display peaks corresponding to non-perovskite phases. The N10 thin films developed a better crystallinity; however, their XRD spectra also show spurious peaks although their intensities are lower than those of the NK00 films. For the NKN thin films grown from 15 mol% K excess precursor solutions (K15), the XRD spectra show many peaks corresponding to non-perovskite phases. The additional spurious peaks are attributable to diffractions assigned to a phase which is richer in potassium, $K_4Nb_6O_{17}$. It is clear that the increase of the Na/K ratio in the precursor solution produces a decrease in the intensity of the peaks corresponding to the $K_4Nb_6O_{17}$ phase. The excess of Na reduces the content of the non-perovskite phase, indicating that the volatilization of Na is larger than K in the films annealed at those temperatures.

Figure 2 shows the SEM microstructure of NKN thin films that were grown using 0 mol% alkaline excess (Fig. 2a) and 20 mol% Na excess (Fig. 2b) precursor solutions, after being annealed at 650 °C. The films grown with the highest Na content exhibit an homogeneous and dense microstructure with grains of about 100 nm in size and with almost a single-modal distribution of grain size, indicating normal grain growth. On the contrary, the NK00

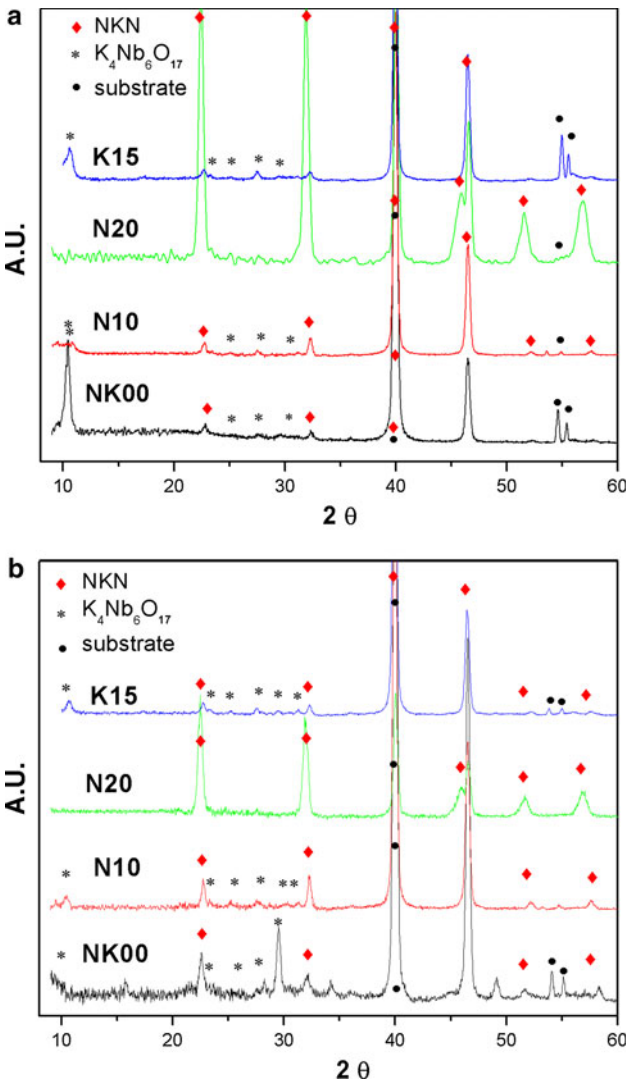

Fig. 1 XRD spectra of the undoped NKN thin films grown using 20 mol% Na excess (N20), 10 mol% Na excess (N10), 0 mol% alkaline excess (NK00) and 15 mol% K excess (K15) in precursor solutions after annealing at 600 °C (**a**) and 700 °C (**b**)

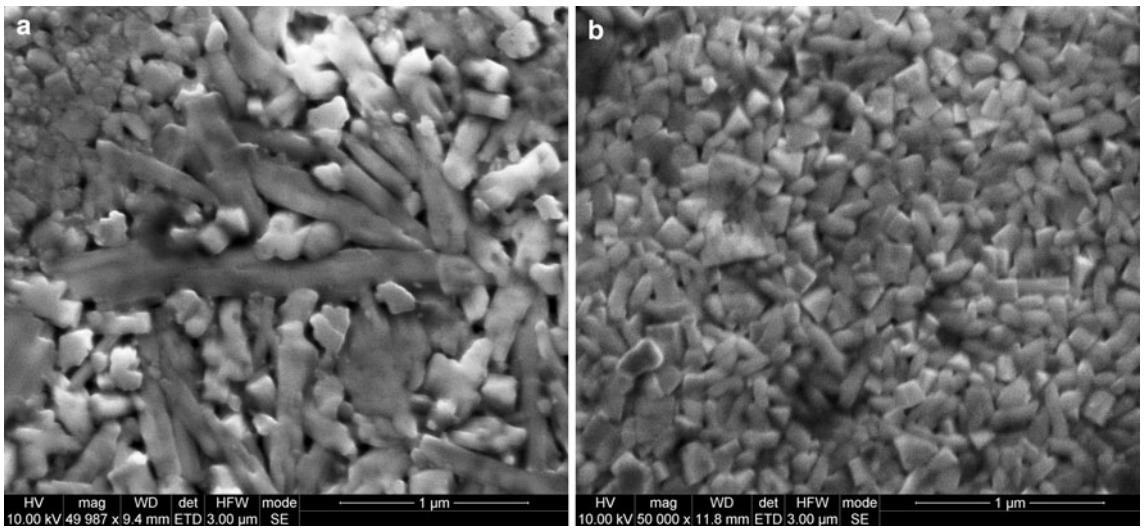

Fig. 2 Scanning electron microscopy micrographs of the thin films grown using **a** 0 mol% alkaline excess, and **b** 20 mol% Na excess annealed at 650 °C

films present a polycrystalline microstructure that consists of two different grain types. We can observe in Fig. 2a the presence of highly anisotropic grains immersed into a fine-grained dense material, with narrow size distribution and equiaxed grain shape. This highly anisotropic grain growth can be related to the fact that the crystallization of these grains does not occur directly from the amorphous precursor but through an asymmetric intermediate crystalline phase; that is, during the heating of the Na-deficient amorphous films, an asymmetric phase is the first to be formed. This is corroborated by the DTA-TG curves shown in Fig. 3. The DTA curve for the N20 composition (Fig. 3b) shows an exothermic sharp peak centered at 565 °C which is attributed to a massive crystallization of NKN occurred during the amorphous-crystalline transition. The DTA curve for the NK00 sample (Fig. 3a) shows, besides an exothermic sharp peak centered at 587 °C, two additional peaks in the temperature range between 500 and 550 °C. One is a small peak at around 509 °C that could be attributed to the crystallization of the $K_4Nb_6O_{17}$ phase. It is known that the $K_4Nb_6O_{17}$ phase appears as the first crystalline phase, during the heating of amorphous precursor gels, around 500 °C [31]. The second exothermic peak centered at 543 °C is probably due to the early formation of part of the NKN perovskite phase induced by reaction of the preexisting $K_4Nb_6O_{17}$ phase with the surrounding amorphous material.

Figure 4 shows the P-E hysteresis loops for NK00, N10, N20 and K15 thin films annealed at 650 °C. The measurements were conducted at a switching frequency of 50 Hz and a maximum applied field of 150 kV/cm. The NK00 and K15 thin films almost do not display ferroelectric behavior, while

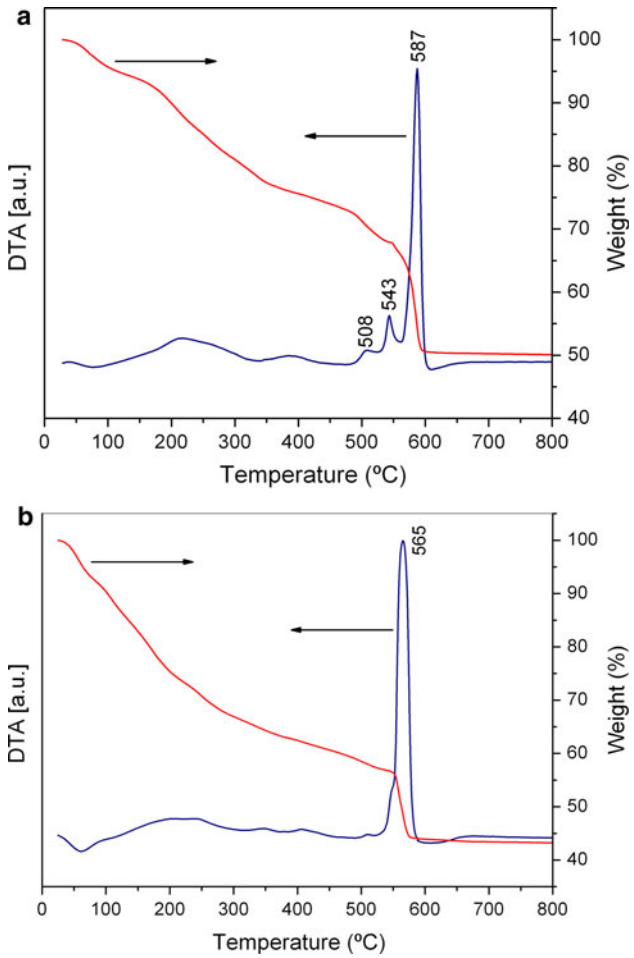

Fig. 3 DTA-TG curves of the gel-powders derived from precursor solutions with **a** 0 mol% alkaline excess, and **b** 20 mol% Na excess

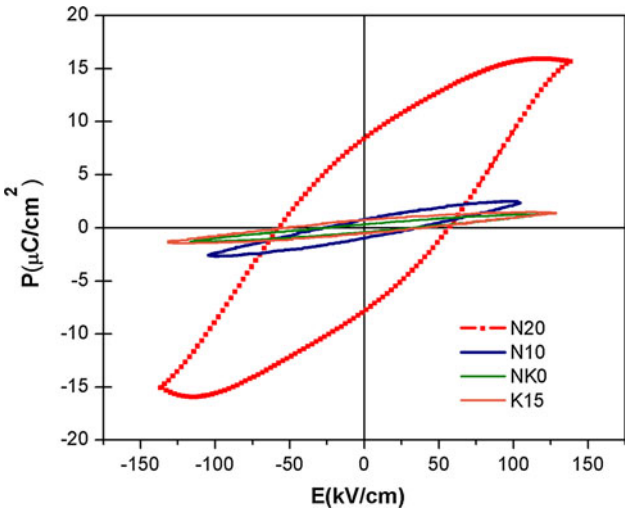

Fig. 4 Ferroelectric P-E hysteresis loops for NKN thin films grown using 20 mol% (N20), 10 mol% Na excess (N10), 0 mol% alkaline excess (NK00) and 15 mol% K excess (K15) in precursor solutions after annealing at 650 °C

the N10 thin film exhibited a very slim ferroelectric hysteresis loop. Only the films grown from the 20 mol% Na excess precursor solution exhibited a well saturated loop, with a relatively high remnant polarization of $P_r = 8.2$ μC/cm^2 and a coercive field of $E_C = 55$ kV/cm. These values are comparable of those obtained by other chemical solution deposition methods which were aided with the addition of Mn to improve sintering [23], which shows the high quality of the developed route.

3.2 Li- and Ta-modified $Na_{0.5}K_{0.5}NbO_3$ thin films

We present now the results obtained for Li- and Ta-doped NKN thin films fabricated with the optimized chelate route. The investigated compositions were $Na_{0.475}K_{0.475}Li_{0.05}NbO_3$ (L5) and $Na_{0.5}K_{0.5}Nb_{0.9}Ta_{0.1}O_3$ (T10), which were chosen in accordance with the optimized composition of the bulk ceramics [15]. We fabricated also samples of composition $Na_{0.475}K_{0.475}Li_{0.05}Nb_{0.9}Ta_{0.1}O_3$ (L5-T10) to compare their structural properties with the other two compositions. Considering the above results, 20 mol% of excess Na precursor was added to the solutions for compensating the evaporation loss. Figure 5 shows the XRD patterns of the L5 (Fig. 5a), T10 (Fig. 5b) and L5-T10 (Fig. 5c) films annealed at different temperatures. It can be seen from those patterns, that all samples annealed at high temperatures presented single perovskite structures, without the presence of spurious phases. This indicates that the system forms a solid solution, that is, Li replaced Na or K in the A site, while Ta replaced Nb in the B site of the perovskite structure. However, the T10 film annealed at 600 °C presents a weak intensity peak at 29.3° (see inset)

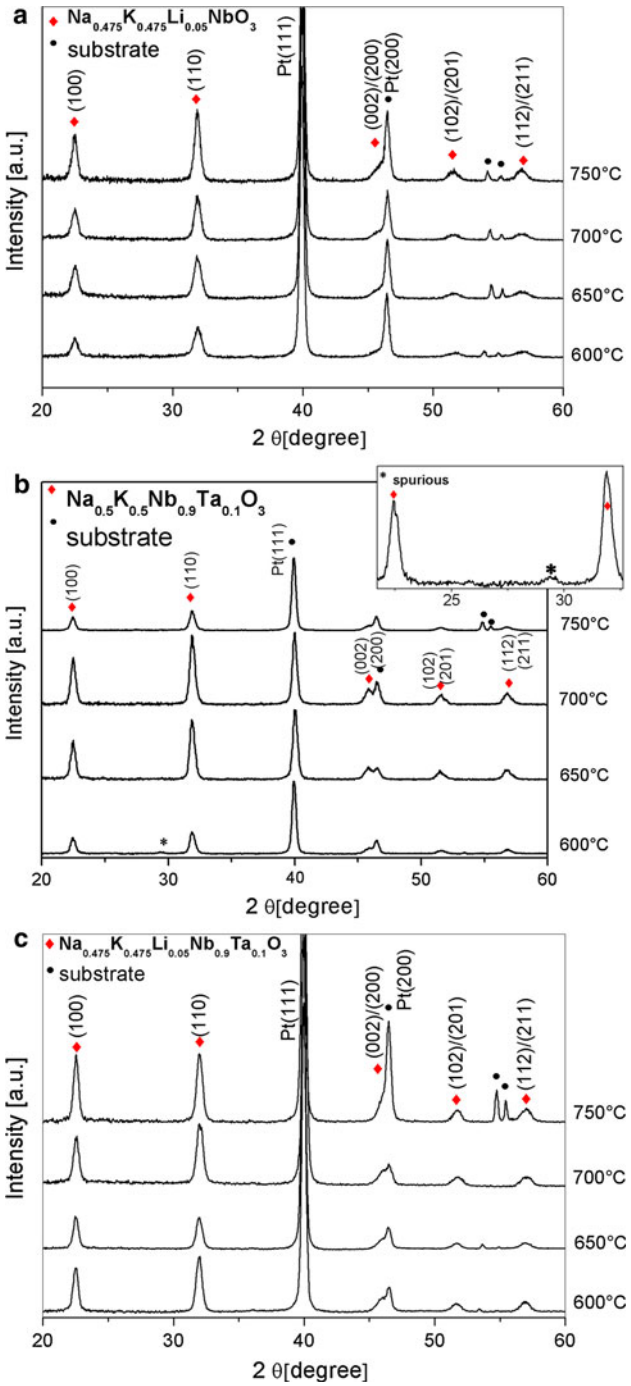

Fig. 5 XRD spectra of $Na_{0.475}K_{0.475}Li_{0.05}NbO_3$ (**a**), $Na_{0.5}K_{0.5}Nb_{0.9}Ta_{0.1}O_3$ (**b**), and $Na_{0.475}K_{0.475}Li_{0.05}Nb_{0.9}Ta_{0.1}O_3$ (**c**) thin films grown on $Pt/TiO_2/SiO_2/Si$ substrate after annealing at different temperatures

indicating the presence of a little trace of secondary phases. Nevertheless, the concentration of this phase decreased with increasing annealing temperature, and a complete crystallization was achieved at 650 °C without any signature of spurious phases. For the case of the L5-T10 films, a peak of weak intensity at 53.4° (which can be assigned to the most intensive peak of $LiTaO_3$) indicates also the

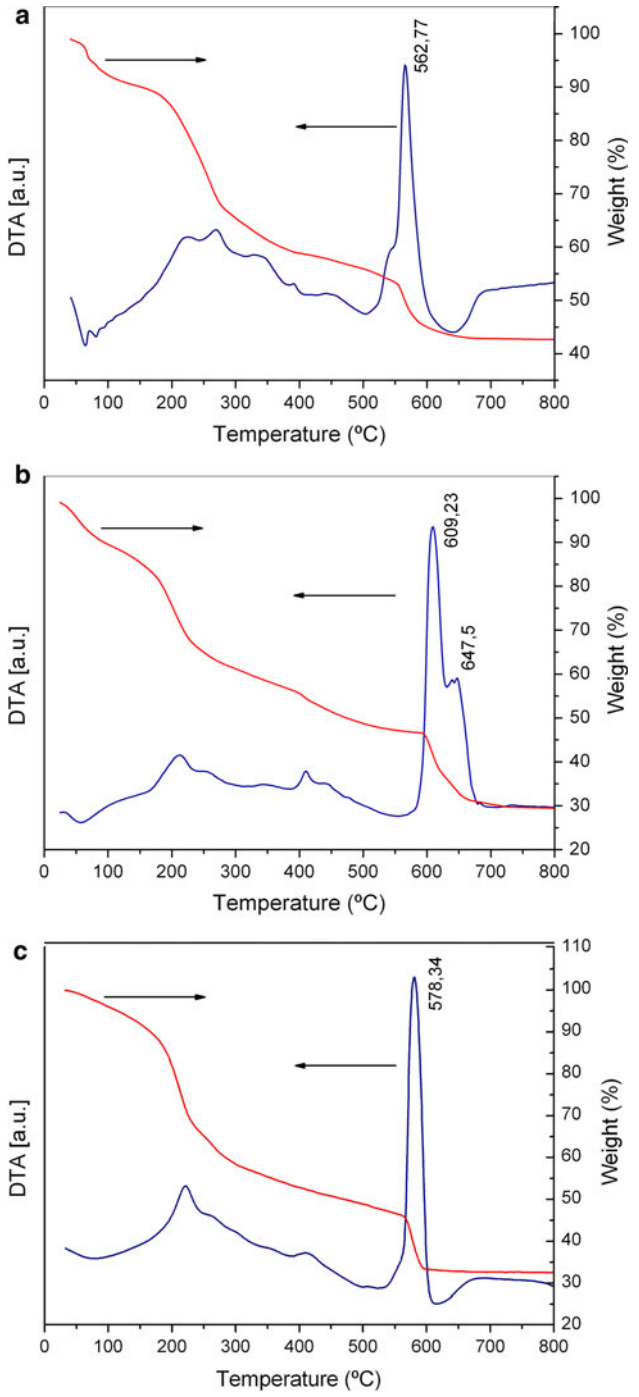

Fig. 6 DTA-TG curves of the gel-powders derived from precursor solutions with **a** 5 % Li doping (L5), **b** 10 % Ta doping (T10), and **c** 5 % Li + 10 % Ta doping (L5-T10)

presence of a secondary phase in the samples annealed at low temperatures.

To analyze the phase formation process, Fig. 6 shows DTA–TGA curves for powders obtained from the precursor solutions which were dried at 200 °C. Roughly speaking, the TGA curves show a constant weight loss assigned to the decomposition and burning of the residual organic groups. The DTA curves display intense exothermic peaks centered near the temperatures where the elimination of the residual organic groups finishes. These peaks are attributed to the elimination of the last organic residues, such as hydroxyls, with a simultaneous onset of the crystallization. The L5 sample exhibits a sharp crystallization peak centered at 562 °C, that is, there is no an appreciable difference with the DTA-TG curve of the undoped sample (Fig. 3b). On the contrary, the DTA curve of the T10 sample exhibits a wider crystallization peak which is in the range 600–650 °C, that is, almost 100 °C above (Fig. 6b). This higher crystallization temperature is possibly related to the refractory properties which presents Tantalum. Precisely, the power to achieve higher sintering temperatures has made this cation useful to manufacture NKN ceramics, so to foster the densification and get a more compact and free of pores structure [32]. Finally, we note that when the system is doped with both cations (L5-T10) the crystallization occurs at a temperature of 578 °C (Fig. 6c), which is more similar to the L5 case.

To analyze to morphology of the films, Fig. 7 shows AFM images of the surfaces of samples thermally treated at 600 and 700 °C. The L5 films display small grains which are separated by clearly defined grain boundaries. The morphology of the grains exhibits a round shape, with an average grain size of around 100 nm for films annealed at 600 °C (Fig. 7a), whereas at 700 °C the grain size grows to 150 nm (Fig. 7b). For the T10 thin films, however, it is noted that the annealed temperature had a pronounced effect on the grain formation. The films annealed at 600 °C display morphological inhomogeneities due to the presence of two different grain sizes, with averages values of 150 and 360 nm (Fig. 7c), which constitutes an additional evidence for the presence of a secondary phase in this composition. The sample treated at 700 °C shows homogeneous microstructure (Fig. 7d), similar to that seen in the lithium-containing composition. A homogeneous microstructure is also observed for samples annealed at 650 °C, indicating that the spurious secondary phase is not longer present in the Ta-doped films annealed at that temperature. As regards the topography of the L5-T10 coatings (not shown here), their microstructures present well-defined grains regardless of the sintering temperature, as the L5 films, with the particularity that the grains are much smaller with a grain size of 70 nm for films annealed at 600 °C. For comparison, we show AFM images for the surfaces of the undoped NKN films (N20) annealed at 600 °C (e) and 700 °C (f).

Figure 8 shows the P-E ferroelectric hysteresis loops for undoped, L5 and T10 thin films annealed at 600 °C (Fig. 8a), 650 °C (Fig. 8b) and 700 °C (Fig. 8c). All films show typical ferroelectric behavior. The hysteresis loop

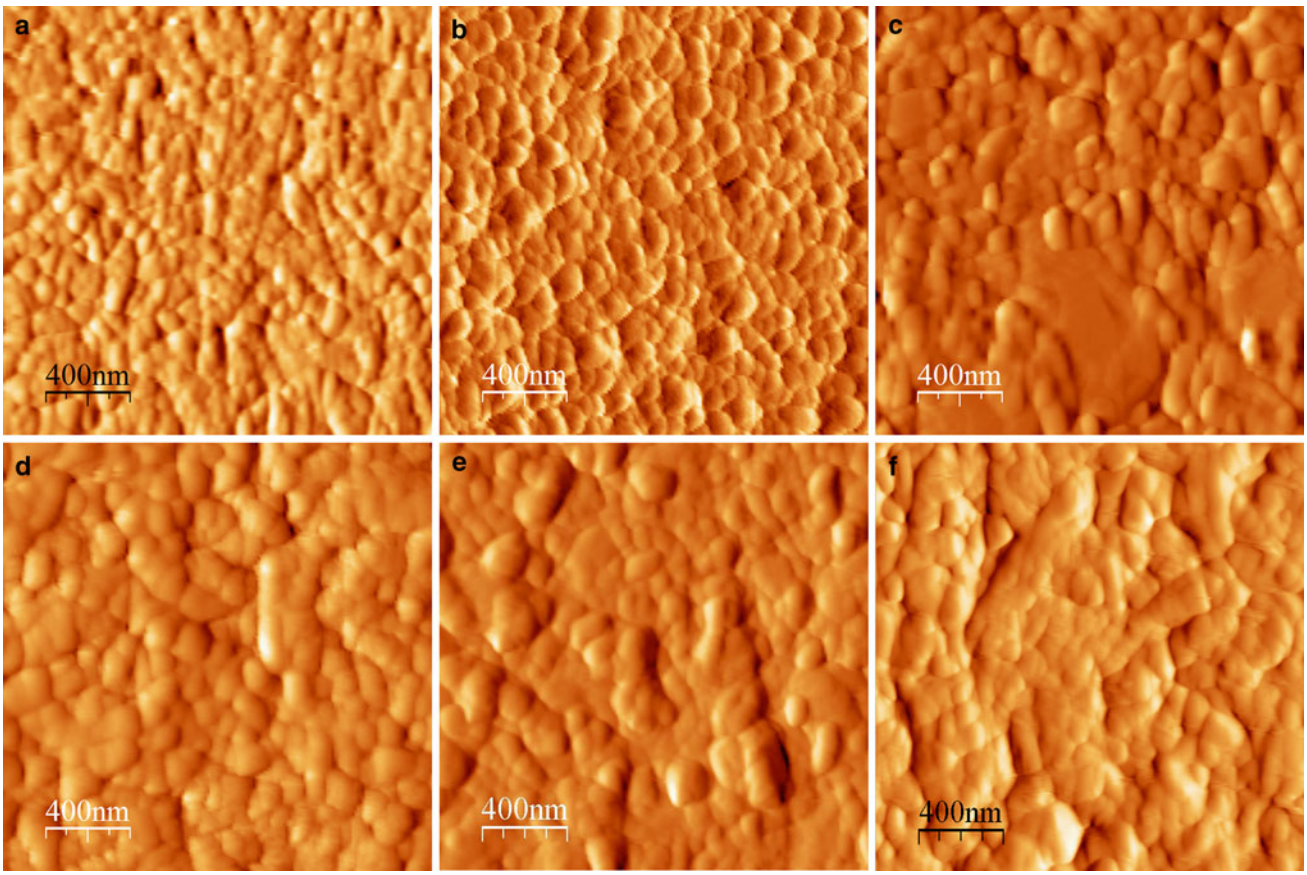

Fig. 7 AFM images for the surfaces of NKN films. $Li_{0.05}Na_{0.475}K_{0.475}NbO_3$ (L5) films annealed at 600 °C (**a**) and 700 °C (**b**). $Na_{0.55}K_{0.5}Ta_{0.1}Nb_{0.9}O_3$ (T10) films annealed at 600 °C (**c**) and 700 °C (**d**). For comparison, we show AFM images for the surfaces of the undoped NKN films (N20) annealed at 600 °C (**e**) and 700 °C (**f**)

for the undoped film annealed at 600 °C is rounded in shape, a signature of the presence of leakage components. However, the doped films annealed at the same temperature display well saturated loops, indicating that Li and Ta additions have a significant influence on the conducting process. The remnant polarizations (P_r) of the undoped, L5 and T10 films annealed at 650 °C are 8, 14 and 17.5 μC/cm^2, respectively; with coercive fields (E_c) of 58, 46 and 30 kV/cm. Both, Ec and Pr increase when the annealed temperature increases. It is clear that both modifications produce a remarkable improvement of the ferroelectric properties. In fact, the P_r values of the doped films are always greater than those of undoped samples. The L5 film, for example, has a remnant polarization of 16 μC/cm^2 at 700 °C, twice the value observed for the NKN sample. We note that the ferroelectric properties of the L5 films presented here are much better that those obtained by other sol–gel methods [33]. It is also interesting to point out that while the remnant polarization of the T10 samples annealed at 650 and 700 °C are greater than those for the L5 films, the opposite occurs for the films annealed at 600 °C. The marked decrease in polarization of the T10 films annealed at low temperature is explained from the presence of a non ferroelectric secondary phase and abnormal grain growth, as was discussed above. The improvement of ferroelectric properties exhibited by the doped films would be related to a lower leakage current, better crystallinity and higher density, as it was found in $Na_{0.5}K_{0.5}Ta_xNb_{1-x}O_3$ ceramics where the grains become denser with the increasing amount of the Ta-doping [34]. Regarding intrinsic factors, since the radius of Nb^{5+} (0.69A) is close to that of Ta^{5+} (0.68A), the increase in the polarization of the T10 film cannot be attributed to a local effect produced by the Ta substitution to Nb. On the contrary, the partial substitution of Ta for Nb decreases both the paraelectric–ferroelectric and tetragonal–orthorhombic phase transition temperatures, weakening the ferroelectricity [35]. In the case of Li-substituted films, however, because of the ion-radius misfit, small lithium ions take off-center positions producing local electric dipole moments, which change their directions with the thermal hopping motions of Li. The

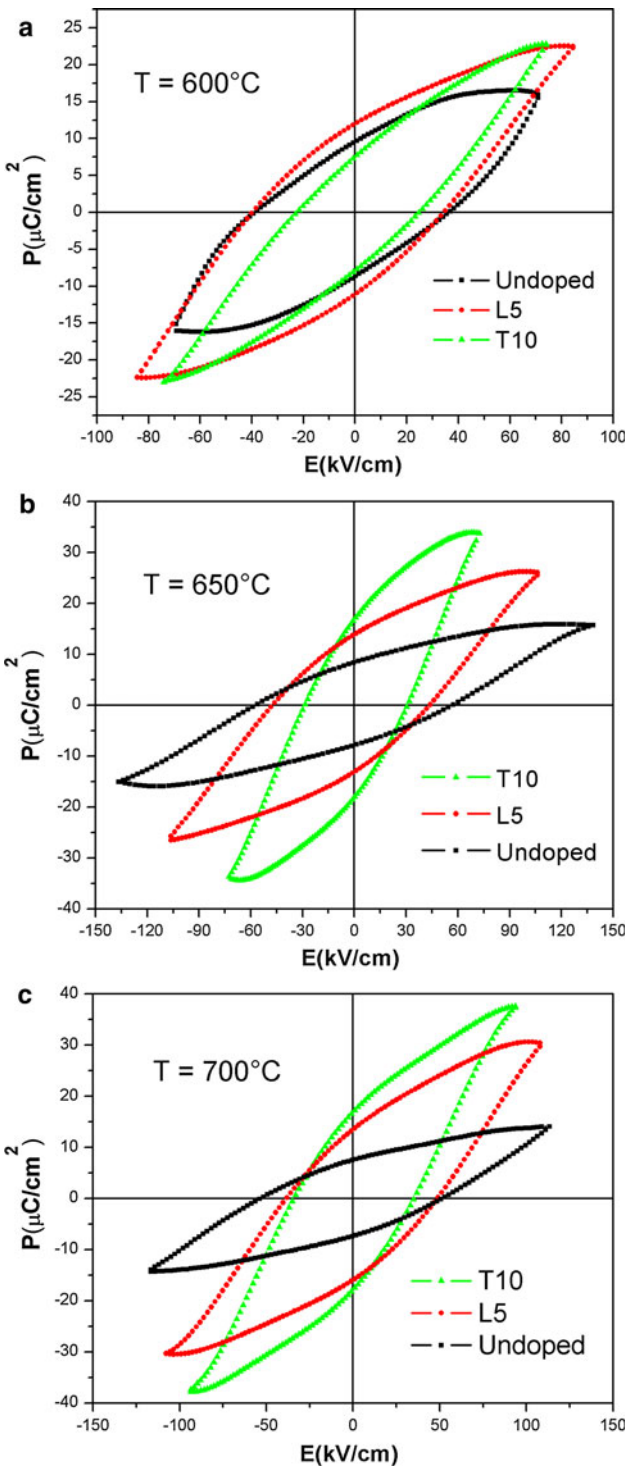

Fig. 8 The P-E hysteresis loops for $Na_{0.5}K_{0.5}NbO_3$ (undoped), $Li_{0.05}Na_{0.475}K_{0.475}NbO_3$ (L5) and $Na_{0.55}K_{0.5}Ta_{0.1}Nb_{0.9}O_3$ (T10) thin films after annealing at 600 °C (**a**), 650 °C (**b**) and 700 °C (**c**)

coupling of these local moments with the ferroelectric host would produce an enhancement of the spontaneous polarization [36].

4 Conclusions

We developed a chelate route for the synthesis of Li- and Ta-modified NKN thin films which offers the advantage of a simple and rapid solution synthesis. The process was optimized by investigating the effect of alkaline volatilization loss on film properties. While no evidence of stoichiometry problems was detected due to potassium volatilization loss, the volatility of Na complicates the growth of phase-pure films. We showed that the addition of a 20 mol% excess of Na chemical to the precursor solution is necessary to compensate volatilization during the heat treatments. In this way, undoped NKN films annealed at 650 °C presented a well crystallized perovskite structure and good ferroelectric properties. We showed that the modification of the films with Li or Ta produce a remarkable improvement of their ferroelectric properties. While undoped films annealed at 600 °C exhibit leakage components, the doped compositions display well saturated hysteresis loops, indicating that Li and Ta additions have a significant influence on the conducting process. NKN film doped with 5 % Li has a remnant polarization of ≈ 16 μC/cm^2 at 700 °C, twice the value obtained for the undoped sample. The doping with 10 % Ta further enhances the renmant polarization of the films due to the development of a homogeneous and high-density microstructure. However, the high crystallization temperature needed for this composition produces abnormal grain growth with the presence of a non-ferroelectric secondary phase at 600 °C, weakening the ferroelectricity of Ta-substituted compositions annealed at low temperatures. We finally hope that the optimized chelate route developed in this work will be useful for a simple and rapid fabrication of other NKN-based thin films with more complex compositions.

Acknowledgments The authors wish to acknowledge financial support from Consejo Nacional de Investigaciones Científicas y Técnicas (CONICET) and Universidad Nacional de Rosario. M.G.S. thanks support from CIUNR.

References

1. Maerder M, Damjanovic D, Setter N (2004) J Electroceram 13:385–392
2. Takenaka T, Nagata H (2005) J Eur Ceram Soc 25:2693–2700
3. Panda PK (2009) J Mater Sci 44:5049–5062
4. Leontsev SO, Eitel RE (2010) Sci Technol Adv Mater 11:044302
5. Lu Y, Li Y (2011) J Adv Dielectr 1:269–288
6. Xiao D (2011) J Adv Dielectr 1(33):40
7. Guo YP, Kakimoto K, Ohsato H (2005) Mater Lett 59:241
8. Kim MS, Jeong SJ, Song JS (2007) J Am Ceram Soc 90:3338
9. Rubio-Marcos F, Ochoa P, Fernandez JF (2007) J Eur Ceram Soc 27:4125
10. Chang YF, Yang ZP, Hou YT, Liu ZH, Wang ZL (2007) Appl Phys Lett 90:232905

11. Saito Y, Takao H (2006) Ferroelectrics 338:1433
12. Yang Z, Chang YF, Liu B, Wei LL (2006) Mater Sci Eng A 432:292
13. Wu JG, Peng T, Wang YY, Xiao DQ, Zhu JM, Jin Y, Zhu J, Yu P, Wu L, Jiang YH (2008) J Am Ceram Soc 91:319
14. Zhang SJ, Xia R, Shrout TR, Zang GZ, Wang JF (2006) J Appl Phys 100:104108
15. Saito Y, Takao H, Tani T, Nonoyama T, Takatori K, Homma T, Nagaya T, Nakamaru M (2004) Nature 84:432
16. Kwak J, Kingon AI, Kim S-H (2012) Mater Lett 82:130–132
17. Saito T, Wada T, Adachi H, Kanno I (2004) Jpn J Appl Phys 43:6627
18. Ryu J, Choi JJ, Hahn BD, Park DS, Yoon WH, Kim KH (2007) Appl Phys Lett 90:152901
19. Lai F, Li J-F (2007) Sol-Gel Sci Tech 42:287
20. Tanaka K, Kakimoto KI, Ohsato H (2006) J Cryst Growth 294:209
21. Kim K-T, Kim G-H, Woo J-C, Kim C-I (2007) Ferroelectrics 356:166–171
22. Nakashima Y, Sakamoto W, Maiwa H, Shimura T, Yogo T (2007) Jpn J Appl Phys 46:L311
23. Wang L, Ren W, Shi P, Chen X, Wu X, Yao X (2010) Appl Phys Lett 97:072902
24. Abazari M, Choi T, Cheong S-W, Safari A (2010) J Phys D Appl Phys 43:025405
25. Ahn CW, Jeong ED, Lee SY, Lee HJ, Kang SH, Kim W III (2008) Appl Phys Lett 93:212905
26. Wang DY, Lin DM, Kwok KW, Chan NY, Dai JY, Li S, Chan HLW (2011) Appl Phys Lett 98:022902
27. Lee SY, Ahn CW, Kim JS, Ullah A, Lee HJ, Hwang H-I, Choi JS, Park BH, Kim W III (2011) J Alloys Compd 509:L194
28. Stachiotti MG, Machado R, Frattini A, Pellegri N, de Sanctis O (2005) J Sol-Gel Sci Technol 36:56–60
29. Machado R, Santiago ML, Stachiotti MG, Frattini A, Pellegri N, Bolmaro R, de Sanctis O (2008) J Sol-Gel Sci Technol 48:294
30. Santiango M, Stachiotti MG, Machado R, Pellegri N, de Sanctis O (2008) Ferroelectrics 370:85
31. Tanaka K, Kakimoto K, Ohsato H (2007) J Eur Ceram Soc 27:3591
32. Zhao P, Zhang B-P, Li J-F (2008) Scripta Mater 58:429–432
33. Lai F, Li J-F, Zhu Z-X, Xu Y (2009) J Appl Phys 106:064101
34. Zhou Y, Guo M, Zhang C, Zhang M (2009) Ceram Int 35:3253–3258
35. Lin D, Kwok KW, Chan HLW (2008) Appl Phys A 91:167
36. Machado R, Sepliarsky M, Stachiotti MG (2012) Phys Rev B 86:094118